DOI: 10.35840/2631-5033/1844

International Journal of
Earth Science and Geophysics

ISSN: 2631-5033

Comparison of Ocean Tide Loading Models Using Strain Data Measured in the Sopronbánfalva Geodynamic Observatory, Hungary

Gyula Mentes*

Geodetic and Geophysical Institute, Research Centre for Astronomy and Earth Sciences, Hungary

Abstract

Tidal strain observations carried out in the Sopronbánfalva Geodynamic Observatory (SGO) in Hungary are used to test thirteen different ocean tide loading models for diurnal and semi-diurnal tidal harmonic constituents O1, K1 and M2. Strain data with one minute sampling rate were corrected for temperature and barometric pressure and decimated to one hour sampling rate. Strain data, corrected in this way, were subjected to correction for ocean load. In the case of the diurnal tidal constituents O1 and K1 the measured amplitude factors of nearly 0.5 became close to the theoretical as a result of the correction, while in the case of the M2 semi diurnal wave the measured amplitude factor of almost 1 hardly changed due to correction. It was only found a negligible difference between the individual global ocean tide loading models mainly due to using different Earth models and Green functions. The effect of the diurnal (O1 and K1) and the semidiurnal (M2) ocean tide loading components is in the same order of magnitude at the SGO. The large residual vectors after the correction suggest that local effects need further investigation.

Keywords

Earth tide, Extensometer, Tidal parameters, Ocean tide loading, Strain

Introduction

Ocean tide surface loading causes both radial and tangential displacements of the Earth surface and changes of gravity. This latter comprises effects resulting from radial displacement in the Earth's gravity field, the internal redistribution of mass, and the direct gravitational attraction of the tidal water mass [1-5].

Various authors have been dealing with testing and comparison of recent global ocean tide models on the basis of gravimetric [6-17], displacement (GPS) [18-25], extensometric [15,16,26,27] and tilt measurements [28-30].

In this paper, the efficiency of ocean loading corrections are compared using thirteen different ocean tide loading models for the diurnal and semi-diurnal tidal harmonic constituents O1, K1 and M2 on the basis of strain data observed in the SGO in 2017.

Measurement Site and Instrument

Extensometric measurements were carried out in the SGO which is located on the Hungarian-Austrian border in the Sopron Mountains. The coordinates of the observatory are: Latitude 47°40’55’’ N; longitude 16°33’32” E; the altitude is 280 m a.s.l. The yearly mean temperature in the gallery is 10.4

***Corresponding author:** *Gyula Mentes, Geodetic and Geophysical Institute, Research Centre for Astronomy and Earth Sciences, Csatkai E. u. 6-8, 9400 Sopron, Hungary, Tel: +36-99-508382*

Accepted: March 16, 2021; **Published:** March 18, 2021

Citation: Mentes G (2021) Comparison of Ocean Tide Loading Models Using Strain Data Measured in the Sopronbánfalva Geodynamic Observatory, Hungary. Int J Earth Sci Geophys 7:044

°C and the yearly and daily temperature variations are less than 0.5 °C and 0.05 °C, respectively. The instrument is a 22 m long quartz-tube extensometer with capacitive transducer. The azimuth of the extensometer is 116°, and its scale factor is 2.093 ± 0.032 nm mV^{-1}. Observation site and construction of the extensometer and its calibration are described in detail by Mentes [31,32].

Data Processing

Strain, temperature and barometric pressure data recorded with a sampling rate of one minute were used for correction by the T-soft program [33]. Data series were despiked and ungapped. The long-term constituent of the strain and temperature data were approximated by fitting a polynomial of 9^{th} order to the raw data series and were subtracted from strain and temperature data, respectively. Theoretical tide was subtracted from the remaining strain data and then strain data were corrected for the temperature and barometric pressure by simple linear regression method and after the correction the theoretical tide was added back. During the correction procedure time lags between strain and temperature and barometric pressure data were taking into consideration. Then the data were low-pass filtered and decimated to one hour sampling and processed by ETERNA 3.40 Earth tide data processing program package [34] using the Wahr-Dehant Earth model [35,36] and the HW95 tidal potential catalogue [37].

For the ocean tide load prediction the SPOTL routines [38] and the ocean load provider service [39] were used. The name of the SPOTL codes are: gr.mmmmmm.www.pnn,c[e|m], The mmmmmm string denotes the Earth model. The SPOTL uses three different Earth models, which are denoted namely the Gutenberg-Bullen Model A average Earth (gbaver) and two extreme models of the Earth's crust and mantle structure [40], one oceanic (gbocen) and one continental shield (gbcont). www denotes: Who computed the function: the source code is wef for W.E. Farrell [1], who computed and tabulated all Green functions. pnn denotes: 01 coarse grid; 02 fine grid (about 20 m for the innermost range) running to much closer to the center (about 100 m). The ce suffix denotes a reference frame with the center of mass of solid Earth and the cm a reference frame with the common center of mass of the load and the Earth.

For ocean load correction of strain data ten ocean tide models have been used with SPOTL, supplemented by the local model osu.mediterranean.2011: EOT11a [41], HAMTIDE11a [42], OSU.TPXO72atlas, OSU.TPXO72, TPX070 [43], DTU10

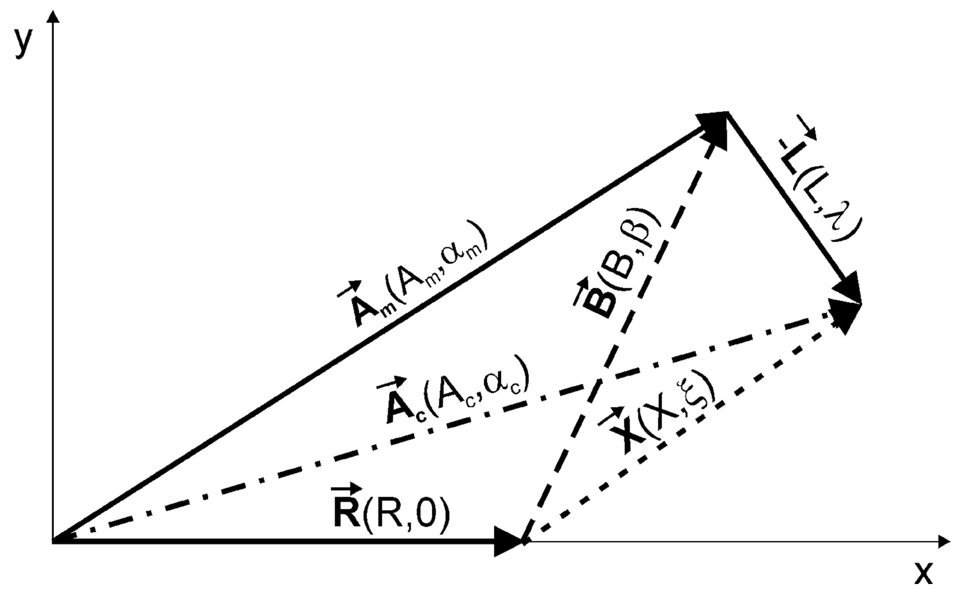

Figure 1: Outline of tidal ocean loading correction. Theoretical tidal vector $\vec{R}(R,\ 0)$, observed tidal vector $\vec{A}_m(A_m,\alpha_m)$, observed residual vector $\vec{B}(B,\beta)$, ocean loading vector $\vec{L}(L,\lambda)$, corrected tidal vector $\vec{A}_c(A_c,\alpha_c)$ and remaining residual vector $\vec{X}(X,\xi)$. The vectors are defined by their amplitudes (R, A_m, B, L, A_c and X) and phases (0, α_m, β, λ, α_c and ξ).

[44], CSR4.0 [45], FES2004 [46], FES95.2.1 [47], SCHW1 [48] and three other models were chosen from the Free Ocean Tide Loading Provider created by Scherneck and Bos (http://holt.oso.chalmers.se/loading/): FES2012 [49], FES2014b [50,51], GOT00.2 [52].

Without external forces the common centre of mass of oceans and the solid Earth will remain fixed in space. Since the ocean tides cause water mass displacements, its centre of mass moves periodically and it is compensated by an opposite motion of the centre of mass of the solid Earth. Accordingly, in these three cases the ocean load was calculated relative to the fixed common mass center of the ocean and the solid Earth and the moving center of mass of the solid Earth. In both cases the calculations were carried out using elastic [1] and visco-elastic Earth model STW105 [53].

The ocean loading correction (see Figure 1) was carried out according to Neumeyer, et al. [54]. The L amplitude and λ phase of the ocean tide load vectors were determined from the above-mentioned different ocean tide loading models and were subtracted from the observed strain tidal vectors $\left(\vec{A}_m\left(A_m,\alpha_m\right)\right)$ in case of the O1, K1 and M2 tidal waves to obtain the corrected tidal strain vectors $\left(\vec{A}_c\left(A_c,\alpha_c\right)\right)$. The remaining residual X depends on the accuracy of the instrument calibration, the local effects, such as the cavity effect, the inaccurately corrected temperature, air pressure and on the accuracy of the ocean tide model.

Results and Discussion

Results of the tidal evaluation of the measured strain data in case of the tidal constituents O1, K1 and M2 without ocean tide loading corrections are shown in Table 1. In the SGO the obtained amplitude factors for the diurnal waves (O1, K1,) are about 0.5, half of the theoretical value, while for the semidiurnal wave M2 it is about 1. Table 2, Table 3, Table 4 and Table 5 show the amplitudes (L) and phases (λ) of the ocean tide load, the amplitudes (A_c) and phases (α_c) of strain corrected for the ocean tide load, the amplitudes (X) and phases (ξ) of the residues and the corrected amplitude factors (η_c) in case of different Earth and global ocean tide loading models.

Table 2 shows the O1 tidal constituents corrected for ocean tide loading with SPOTL in case of different Earth models and 10 global ocean tide models. The uncorrected amplitude factor is 0.5323 (see Table 1), while the corrected amplitude factors (average: 1.025 ± 0.001) are somewhat higher than one in the case of solid Earth model with the center of mass (ce suffix denotes the reference frame with the center of mass of solid Earth) and somewhat lower (average: 0.928 ± 0.003) in the case of the Earth model with the common center of mass of the load and the Earth (cm suffix denotes the reference frame with the common center of mass of the load and the Earth). Similar results were obtained for K1 (see Table 3) for which the uncorrected amplitude factor was 0.5283. The corrected average amplitude factors are 1.026 ± 0.001 (ce) and 0.966 ± 0.002 (cm). The measured amplitude factor for M2 is 1.0036 (see Table 1), while the corrected average values (see Table 4) are 1.059 ± 0.004 (ce) and 1.039 ± 0.007 (cm). In both cases the corrected values are higher than the measured value, but similarly to O1 and K1 the corrected values are higher in case of reference frame with the center of Earth (ce) than in the case of common center of load mass and the center of Earth.

Table 5 shows the results of correction of the O1, K1, M2 waves for ocean tide loading derived from three ocean loading models (FS2012, FS214b and GOT00.2) with different Earth models calculated by the ocean load provider service. In case of the elastic and visco-elastic Earth models almost identical corrected amplitude factors (η_c) were obtained for O1, K1 and M2 waves but these were some-

Table 1: Tidal results calculated from strain data corrected for temperature and barometric pressure.

Wave	Theoretical amplitude R [nstr]	Measured amplitude A_m [nstr]	Measured phase lag α_m [degree]	Amplitude factor η	Measured residual B [nstr]	Phase of the residual β [degree]
O1	6.5932	3.5098	-6.3118	0.5323	3.1286	187.0846
K1	9.2690	4.8964	-3.4378	0.5283	4.3912	183.8339
M2	5.0573	5.0754	-14.4836	1.0036	1.2768	263.6103

Table 2: Results of correction of the O1 wave for ocean tide loading derived from 10 ocean loading models with different Earth models calculated by SPOTL routines. The observed values, not corrected for ocean tide loading, are in Table 1.

Earth model	Ocean tide model	Amplitude of the ocean tide load	Phase of the ocean tide load	Corrected strain amplitude.	Phase of the corrected strain	Amplitude of the remaining residual	Phase of the remaining residual	Corrected amplitude factor
		L [nstr]	λ [degree]	A_c [nstr]	α_c [degree]	X [nstr]	ξ [degree]	η_c
gbocen.ce	eot11a	0.182	37.869	6.777	4.168	3.286	8.621	1.028
	hamtide11a	0.159	38.559	6.756	4.072	3.265	8.451	1.025
	osu.tpxo72atlas	0.160	42.219	6.751	4.149	3.261	8.616	1.024
	tpxo70	0.170	40.758	6.761	4.170	3.271	8.645	1.026
	fes952	0.173	39.506	6.767	4.163	3.276	8.623	1.026
	fes2004	0.160	39.651	6.756	4.102	3.265	8.513	1.025
	osu.tpxo72	0.164	41.468	6.756	4.154	3.265	8.620	1.025
	dtu10tr	0.164	39.949	6.758	4.125	3.267	8.557	1.025
	csr4tr	0.166	39.345	6.761	4.123	3.270	8.549	1.025
	schw1	0.150	38.033	6.750	4.022	3.258	8.356	1.024
gbav.ce	eot11a	0.168	41.242	6.759	4.169	3.268	8.647	1.025
	hamtide11a	0.160	38.749	6.757	4.082	3.266	8.470	1.025
	osu.tpxo72atlas	0.161	42.407	6.752	4.159	3.261	8.635	1.024
	tpxo70	0.171	40.899	6.762	4.180	3.272	8.664	1.026
	fes952	0.175	39.612	6.768	4.172	3.277	8.641	1.026
	fes2004	0.162	39.830	6.757	4.112	3.266	8.532	1.025
	osu.tpxo72	0.165	41.635	6.756	4.164	3.266	8.640	1.025
	dtu10tr	0.165	40.109	6.759	4.135	3.268	8.575	1.025
	csr4tr	0.167	39.491	6.762	4.133	3.271	8.568	1.026
	schw1	0.152	38.319	6.751	4.034	3.259	8.379	1.024
gbcont.ce	eot11a	0.166	42.862	6.755	4.191	3.264	8.698	1.024
	hamtide11a	0.158	40.370	6.753	4.104	3.262	8.521	1.024
	osu.tpxo72atlas	0.160	44.211	6.748	4.185	3.257	8.694	1.023
	tpxo70	0.169	42.506	6.758	4.204	3.268	8.719	1.025
	fes952	0.173	41.107	6.764	4.195	3.273	8.694	1.026
	fes2004	0.160	41.516	6.753	4.137	3.262	8.588	1.024
	osu.tpxo72	0.163	43.419	6.752	4.189	3.261	8.698	1.024
	dtu10tr	0.163	41.752	6.755	4.158	3.264	8.629	1.025
	csr4tr	0.166	41.165	6.758	4.160	3.267	8.629	1.025
	schw1	0.149	39.987	6.746	4.054	3.255	8.426	1.023
Average		0.164	40.618	6.757	4.139	3.266	8.587	1.025
STD		0.007	1.582	0.006	0.047	0.006	0.094	0.001

gbocen. cm	eot11a	0.624	148.167	6.127	6.665	2.672	15.434	0.929
	hamtide11a	0.621	149.556	6.119	6.537	2.663	15.168	0.928
	osu.tpxo72atlas	0.635	147.751	6.121	6.761	2.668	15.670	0.928
	tpxo70	0.636	149.075	6.111	6.660	2.656	15.476	0.927
	fes952	0.652	153.129	6.072	6.397	2.613	15.002	0.921
	fes2004	0.622	148.183	6.128	6.650	2.673	15.396	0.929
	osu.tpxo72	0.634	147.915	6.120	6.744	2.667	15.635	0.928
	dtu10tr	0.624	147.928	6.129	6.680	2.674	15.462	0.930
	csr4tr	0.618	148.323	6.130	6.618	2.674	15.316	0.930
	schw1	0.595	148.262	6.148	6.490	2.690	14.970	0.933
gbav.cm	eot11a	0.624	148.030	6.127	6.675	2.673	15.455	0.929
	hamtide11a	0.621	149.428	6.120	6.547	2.664	15.189	0.928
	osu.tpxo72atlas	0.635	147.633	6.122	6.771	2.669	15.691	0.928
	tpxo70	0.636	148.945	6.112	6.671	2.657	15.497	0.927
	fes952	0.651	152.994	6.073	6.407	2.615	15.022	0.921
	fes	0.622	148.056	6.129	6.660	2.674	15.417	0.930
	osu.tpxo72	0.634	147.788	6.121	6.755	2.668	15.657	0.928
	dtu10tr	0.624	147.800	6.130	6.690	2.675	15.482	0.930
	csr4tr	0.618	148.184	6.131	6.628	2.676	15.337	0.930
	schw1	0.595	148.221	6.149	6.491	2.691	14.970	0.933
gbcont.cm	eot11a	0.629	148.071	6.123	6.701	2.669	15.528	0.929
	hamtide11a	0.626	149.448	6.116	6.573	2.660	15.261	0.928
	osu.tpxo72atlas	0.640	147.646	6.118	6.801	2.665	15.773	0.928
	tpxo70	0.641	148.954	6.108	6.699	2.654	15.574	0.926
	fes952	0.656	152.976	6.069	6.434	2.611	15.096	0.920
	fes2004	0.627	148.052	6.125	6.690	2.671	15.496	0.929
	osu.tpxo72	0.640	147.812	6.117	6.784	2.664	15.738	0.928
	dtu10tr	0.629	147.834	6.125	6.717	2.671	15.556	0.929
	csr4tr	0.623	148.162	6.127	6.659	2.672	15.420	0.929
	schw1	0.601	148.180	6.145	6.526	2.688	15.062	0.932
Average		0.628	148.750	6.120	6.636	2.665	15.392	0.928
STD		0.014	1.522	0.019	0.110	0.019	0.234	0.003

what higher when motion correction was applied in case of the diurnal waves (O1 and K1), while for the semidiurnal wave M2 the opposite values were obtained.

Comparing the residues in Table 2, Table 3, Table 4 and Table 5, it can be seen that the amplitudes (*X*) of the residual vectors changed only slightly compared to the measured ones (*B*), while the phase angles decreased significantly. Large residues remaining after the correction suggest that local effects (e.g. cavity) affect the measurement site, which requires further study. The amplitudes (*L*) of the ocean load vectors are in the same order of magnitude for the diurnal (O1, K1) and semidiurnal (M2) waves at the site of the SGO.

Conclusions

Strain measurement was used to test thirteen global ocean tide loading models. Tidal parameters corrected for ocean tide loading were calculated. All models provided virtually the same result. In the case of the diurnal tidal constituents O1 and K1 the measured amplitude factors of nearly 0.5 became close to 1 as a result of the correction, while in the

Table 3: Results of correction of the K1 wave for ocean tide loading derived from 10 ocean loading models with different Earth models calculated by SPOTL routines. The observed values, not corrected for ocean tide loading, are in Table 1.

Earth model	Ocean tide model	Amplitude of the ocean tide load	Phase of the ocean tide load	Corrected strain amplitude.	Phase of the corrected strain	Amplitude of the remaining residual	Phase of the remaining residual	Corrected amplitude factor
		L [nstr]	λ [degree]	A_c [nstr]	α_c [degree]	X [nstr]	ξ [degree]	η_c
gbocen.ce	eot11a	0.282	35.946	9.518	2.724	4.633	5.604	1.027
	hamtide11a	0.278	37.321	9.510	2.744	4.626	5.649	1.026
	osu. tpxo72atlas	0.283	38.759	9.511	2.797	4.626	5.757	1.026
	tpxo70	0.280	38.125	9.510	2.770	4.625	5.703	1.026
	fes952	0.268	38.863	9.498	2.745	4.613	5.659	1.025
	fes2004	0.289	34.997	9.525	2.721	4.640	5.592	1.028
	osu.tpxo72	0.284	37.139	9.516	2.761	4.631	5.680	1.027
	dtu10tr	0.282	36.704	9.515	2.741	4.630	5.640	1.027
	csr4tr	0.247	35.234	9.489	2.591	4.603	5.347	1.024
	schw1	0.272	37.912	9.504	2.736	4.619	5.637	1.025
gbav.ce	eot11a	0.286	35.999	9.521	2.738	4.636	5.631	1.027
	hamtide11a	0.278	37.770	9.509	2.755	4.625	5.673	1.026
	osu. tpxo72atlas	0.284	39.223	9.509	2.809	4.625	5.782	1.026
	tpxo70	0.280	38.550	9.509	2.781	4.624	5.726	1.026
	fes952	0.268	39.304	9.497	2.754	4.612	5.679	1.025
	fes2004	0.289	35.436	9.524	2.732	4.639	5.616	1.028
	osu.tpxo72	0.285	37.578	9.515	2.772	4.630	5.704	1.027
	dtu10tr	0.282	37.116	9.514	2.752	4.629	5.663	1.026
	csr4tr	0.247	35.577	9.489	2.598	4.603	5.362	1.024
	schw1	0.272	38.241	9.503	2.745	4.618	5.656	1.025
gbcont.ce	eot11a	0.294	37.792	9.522	2.810	4.638	5.777	1.027
	hamtide11a	0.287	39.538	9.511	2.827	4.627	5.818	1.026
	osu. tpxo72atlas	0.292	40.906	9.511	2.879	4.627	5.927	1.026
	tpxo70	0.289	40.287	9.510	2.853	4.626	5.872	1.026
	fes952	0.276	41.172	9.498	2.827	4.613	5.827	1.025
	fes2004	0.296	37.265	9.526	2.805	4.641	5.764	1.028
	osu.tpxo72	0.293	39.304	9.517	2.844	4.633	5.851	1.027
	dtu10tr	0.290	38.983	9.515	2.825	4.631	5.812	1.027
	csr4tr	0.255	37.607	9.491	2.672	4.606	5.514	1.024
	schw1	0.280	40.052	9.504	2.816	4.620	5.800	1.025
Average		0.280	37.957	9.510	2.764	4.625	5.691	1.026
STD		0.012	1.631	0.010	0.064	0.010	0.129	0.001

gbocen.cm	eot11a	0.594	125.246	8.969	4.939	4.113	10.823	0.968
	hamtide11a	0.609	127.707	8.940	4.934	4.083	10.855	0.964
	osu.tpxo72atlas	0.633	124.868	8.953	5.169	4.101	11.345	0.966
	tpxo70	0.637	126.095	8.940	5.145	4.087	11.313	0.964
	fes952	0.643	125.980	8.938	5.185	4.085	11.402	0.964
	fes2004	0.604	123.544	8.980	5.052	4.125	11.051	0.969
	osu.tpxo72	0.628	125.726	8.948	5.112	4.094	11.231	0.965
	dtu10tr	0.610	123.997	8.973	5.069	4.118	11.099	0.968
	csr4tr	0.604	125.757	8.960	4.975	4.104	10.914	0.967
	schw1	0.545	127.238	8.978	4.610	4.116	10.096	0.969
gbav.cm	eot11a	0.596	125.250	8.968	4.950	4.112	10.848	0.968
	hamtide11a	0.611	127.697	8.938	4.946	4.082	10.883	0.964
	osu.tpxo72atlas	0.635	124.862	8.952	5.182	4.100	11.374	0.966
	tpxo70	0.639	126.080	8.939	5.157	4.086	11.341	0.964
	fes952	0.645	125.999	8.936	5.195	4.084	11.427	0.964
	fes2004	0.606	123.552	8.979	5.063	4.124	11.078	0.969
	osu.tpxo72	0.630	125.723	8.946	5.125	4.093	11.259	0.965
	dtu10tr	0.612	123.987	8.972	5.081	4.118	11.126	0.968
	csr4tr	0.605	125.751	8.959	4.983	4.103	10.933	0.967
	schw1	0.547	127.194	8.977	4.619	4.116	10.116	0.969
gbcont.cm	eot11a	0.605	124.525	8.970	5.026	4.115	11.011	0.968
	hamtide11a	0.620	126.952	8.941	5.022	4.085	11.044	0.965
	osu.tpxo72atlas	0.644	124.198	8.954	5.257	4.103	11.533	0.966
	tpxo70	0.648	125.391	8.941	5.233	4.089	11.503	0.965
	fes952	0.654	125.350	8.938	5.271	4.087	11.590	0.964
	fes2004	0.616	122.875	8.981	5.140	4.127	11.241	0.969
	osu.tpxo72	0.640	125.007	8.949	5.201	4.096	11.422	0.965
	dtu10tr	0.622	123.339	8.973	5.158	4.120	11.291	0.968
	csr4tr	0.614	124.945	8.962	5.061	4.107	11.098	0.967
	schw1	0.556	126.416	8.979	4.694	4.118	10.278	0.969
Average		0.615	125.375	8.958	5.052	4.103	11.084	0.966
STD		0.027	1.189	0.016	0.163	0.014	0.365	0.002

case of the M2 semi diurnal wave, the measured amplitude factor of almost 1 hardly changed due to correction. It was only found a negligible difference between the individual tide loading models mainly due to the use of different Earth models, and Green functions. The effect of the diurnal (O1 and K1) and the semidiurnal (M2) ocean tide loading components is in the same order of magnitude at the SGO. The large residual vectors after the correction suggest that local effects need further investigation.

Acknowledgments

This work was funded by the Hungarian National Research Fund (OTKA) under project K 109060. Special thanks to Tibor Molnár for his careful maintenance of the instruments.

Table 4: Results of correction of the M2 wave for ocean tide loading derived from 10 ocean loading models with different Earth models calculated by SPOTL routines. The observed values, not corrected for ocean tide loading, are in Table 1.

Earth model	Ocean tide model	Amplitude of the ocean tide load	Phase of the ocean tide load	Corrected strain amplitude.	Phase of the corrected strain	Amplitude of the remaining residual	Phase of the remaining residual	Corrected amplitude factor
		L [nstr]	λ [degree]	A_c [nstr]	α_c [degree]	X [nstr]	ξ [degree]	η_c
gbocen.ce	eot11a	0.155	112.319	5.351	15.308	1.415	86.548	1.058
	hamtide11a	0.164	114.788	5.343	15.389	1.419	86.953	1.057
	osu. tpxo72atlas	0.149	106.327	5.368	15.255	1.415	85.859	1.061
	tpxo70	0.166	111.617	5.352	15.429	1.426	86.668	1.058
	fes952	0.159	102.631	5.378	15.361	1.428	85.611	1.063
	fes2004	0.182	114.356	5.342	15.589	1.437	87.252	1.056
	osu.tpxo72	0.149	111.685	5.354	15.249	1.410	86.386	1.059
	dtu10tr	0.169	110.058	5.356	15.464	1.430	86.548	1.059
	csr4tr	0.157	112.819	5.350	15.329	1.416	86.635	1.058
	schw1	0.100	93.336	5.391	14.713	1.376	84.231	1.066
gbav.ce	eot11a	0.169	116.631	5.337	15.434	1.421	87.244	1.055
	hamtide11a	0.178	118.733	5.329	15.512	1.426	87.643	1.054
	osu. tpxo72atlas	0.161	111.146	5.354	15.377	1.422	86.535	1.059
	tpxo70	0.181	115.899	5.337	15.566	1.433	87.399	1.055
	fes952	0.170	107.098	5.365	15.479	1.434	86.239	1.061
	fes2004	0.198	117.769	5.328	15.727	1.444	87.934	1.053
	osu.tpxo72	0.162	116.492	5.339	15.366	1.416	87.099	1.056
	dtu10tr	0.182	114.138	5.342	15.586	1.436	87.220	1.056
	csr4tr	0.170	116.906	5.336	15.445	1.422	87.295	1.055
	schw1	0.111	103.464	5.374	14.851	1.382	85.092	1.063
gbcont.ce	eot11a	0.138	110.542	5.358	15.125	1.401	86.076	1.059
	hamtide11a	0.147	113.334	5.350	15.214	1.406	86.492	1.058
	osu. tpxo72atlas	0.132	102.679	5.376	15.076	1.402	85.294	1.063
	tpxo70	0.151	109.519	5.359	15.268	1.414	86.197	1.060
	fes952	0.142	99.686	5.384	15.173	1.414	85.122	1.065
	fes2004	0.165	112.531	5.350	15.409	1.423	86.737	1.058
	osu.tpxo72	0.132	109.279	5.361	15.066	1.397	85.868	1.060
	dtu10tr	0.151	107.570	5.364	15.273	1.416	86.007	1.061
	csr4tr	0.140	111.062	5.356	15.151	1.402	86.165	1.059
	schw1	0.089	83.787	5.403	14.553	1.366	83.536	1.068
Average		0.154	109.607	5.356	15.291	1.415	86.329	1.059
STD		0.024	7.414	0.018	0.252	0.018	0.963	0.004

gbocen.cm	eot11a	1.052	-88.895	5.246	2.365	0.273	52.501	1.037
	hamtide11a	1.063	-88.339	5.256	2.248	0.271	49.416	1.039
	osu.tpxo72atlas	1.048	-86.308	5.293	2.415	0.309	46.284	1.047
	tpxo70	1.034	-87.026	5.280	2.562	0.309	49.807	1.044
	fes952	1.072	-92.569	5.177	2.187	0.220	63.672	1.024
	fes2004	1.049	-89.331	5.238	2.402	0.271	54.251	1.036
	osu.tpxo72	1.044	-86.196	5.295	2.457	0.313	46.550	1.047
	dtu10tr	1.082	-88.332	5.256	2.038	0.258	46.507	1.039
	csr4tr	1.063	-88.323	5.256	2.250	0.272	49.400	1.039
	schw1	0.927	-86.576	5.288	3.728	0.398	59.695	1.046
gbav.cm	eot11a	1.045	-89.809	5.230	2.455	0.269	56.327	1.034
	hamtide11a	1.055	-89.241	5.240	2.334	0.267	53.177	1.036
	osu.tpxo72atlas	1.040	-87.177	5.277	2.502	0.303	49.466	1.044
	tpxo70	1.025	-87.996	5.263	2.660	0.304	53.371	1.041
	fes952	1.066	-93.404	5.162	2.275	0.221	68.050	1.021
	fes2004	1.041	-90.249	5.222	2.504	0.268	58.227	1.033
	osu.tpxo72	1.036	-87.122	5.278	2.536	0.306	49.735	1.044
	dtu10tr	1.074	-89.197	5.240	2.125	0.252	50.366	1.036
	csr4tr	1.056	-89.181	5.241	2.331	0.267	52.950	1.036
	schw1	0.918	-87.797	5.268	3.830	0.396	62.792	1.042
gbcont.cm	eot11a	1.067	-88.337	5.256	2.200	0.268	48.771	1.039
	hamtide11a	1.077	-87.798	5.266	2.091	0.268	45.742	1.041
	osu.tpxo72atlas	1.063	-85.664	5.306	2.258	0.308	42.756	1.049
	tpxo70	1.047	-86.465	5.291	2.421	0.307	46.730	1.046
	fes952	1.087	-91.959	5.187	2.014	0.212	59.191	1.026
	fes2004	1.063	-88.686	5.250	2.244	0.267	50.369	1.038
	osu.tpxo72	1.059	-85.614	5.307	2.294	0.311	43.125	1.049
	dtu10tr	1.098	-87.705	5.268	1.870	0.256	42.161	1.042
	csr4tr	1.077	-87.777	5.267	2.090	0.268	45.667	1.041
	schw1	0.939	-85.675	5.302	3.593	0.396	56.918	1.048
Average		1.046	-88.292	5.257	2.443	0.287	51.799	1.039
STD		0.043	1.907	0.035	0.460	0.045	6.370	0.007

Table 5: Results of correction of the O1, K1, M2 waves for ocean tide loading derived from three ocean loading models with different Earth models calculated by the ocean load provider service. L amplitude of the ocean tide load, λ phase of the ocean tide load, A_c corrected strain amplitude, α_c phase of the corrected strain, X amplitude of the remaining residual, ξ phase of the remaining residual, η_c corrected amplitude factor. The observed values, not corrected for ocean tide loading, are in Table 1.

Tidal wave		Ocean tide model	Earth model	Motion correction	L [nstr]	λ [degree]	A_c [nstr]	α_c [degree]	X [nstr]	ξ [degree]	η_c
O1		FS2012	Elastic Farrel	No	0.175	78.829	3.187	6.993	6.685	3.328	1.014
		FS214b			0.165	81.586	3.176	6.993	6.674	3.322	1.012
		GOT00.2			0.091	46.008	3.200	6.993	6.697	3.335	1.016
		FS2012	Visco-elastic		0.165	81.586	3.176	6.993	6.674	3.322	1.012
		FS214b			0.165	81.586	3.176	6.993	6.674	3.322	1.012
		GOT00.2			0.089	40.081	3.203	6.993	6.701	3.337	1.016
	Average				0.142	68.279	3.186	6.993	6.684	3.328	1.014
	STD				0.037	17.952	0.011	0.000	0.011	0.006	0.002
		FS2012	Elastic Farrel	Yes	0.728	63.731	3.580	6.993	7.077	3.531	1.073
		FS214b			0.805	63.158	3.639	6.993	7.135	3.560	1.082
		GOT00.2			0.645	59.295	3.560	6.993	7.057	3.522	1.070
		FS2012	Visco-elastic		0.727	63.903	3.578	6.993	7.074	3.530	1.073
		FS214b			0.805	63.158	3.639	6.993	7.135	3.560	1.082
		GOT00.2			1.917	82.483	4.059	6.993	7.555	3.751	1.146
	Average				0.938	65.955	3.676	6.993	7.172	3.576	1.088
	STD				0.441	7.554	0.174	0.000	0.174	0.080	0.026
K1		FS2012	Elastic Farrel	No	0.172	16.539	4.559	3.743	9.450	1.805	1.020
		FS214b			0.179	13.154	4.568	3.743	9.460	1.806	1.021
		GOT00.2			0.292	71.656	4.509	3.743	9.401	1.794	1.014
		FS2012	Visco-elastic		0.172	16.539	4.559	3.743	9.450	1.805	1.020
		FS214b			0.165	81.586	3.176	6.993	6.674	3.322	1.012
		GOT00.2			0.089	40.081	3.203	6.993	6.701	3.337	1.016
	Average				0.178	39.926	4.096	4.826	8.523	2.312	1.017
	STD				0.059	27.547	0.641	1.532	1.298	0.720	0.003
		FS2012	Elastic Farrel	Yes	0.505	34.408	4.833	3.743	9.724	1.859	1.049
		FS214b			0.805	63.158	3.639	6.993	7.135	3.560	1.082
		GOT00.2			0.645	59.295	3.560	6.993	7.057	3.522	1.070
		FS2012	Visco-elastic		0.505	34.408	4.833	3.743	9.724	1.859	1.049
		FS214b			0.805	63.158	3.639	6.993	7.135	3.560	1.082
		GOT00.2			1.917	82.483	4.059	6.993	7.555	3.751	1.146
	Average				0.864	56.152	4.094	5.910	8.055	3.019	1.080
	STD				0.487	17.063	0.547	1.532	1.191	0.823	0.033

M2		FS2012	Elastic Farrel	No	0.553	-51.488	0.969	83.519	5.274	10.522	1.043
		FS214b			0.566	-52.518	0.955	83.519	5.270	10.376	1.042
		GOT00.2			0.571	44.475	1.757	83.519	5.556	18.323	1.099
		FS2012	Visco-elastic		0.553	-51.488	0.969	83.519	5.274	10.522	1.043
		FS214b			0.566	-52.518	0.955	83.519	5.270	10.376	1.042
		GOT00.2			0.587	48.649	1.790	83.519	5.570	18.630	1.101
	Average				0.566	-19.148	1.233	83.519	5.369	13.125	1.062
	STD				0.012	46.482	0.383	0.000	0.137	3.786	0.027
		FS2012	Elastic Farrel	Yes	0.750	-89.675	0.539	83.519	5.165	5.959	1.021
		FS214b			0.849	-88.080	0.455	83.519	5.147	5.040	1.018
		GOT00.2			0.767	-87.871	0.531	83.519	5.163	5.870	1.021
		FS2012	Visco-elastic		0.750	-89.675	0.539	83.519	5.165	5.959	1.021
		FS214b			0.849	-88.080	0.455	83.519	5.147	5.040	1.018
		GOT00.2			1.031	66.615	2.283	83.519	5.797	23.047	1.146
	Average				0.833	-62.794	0.800	83.519	5.264	8.486	1.041
	STD				0.098	57.878	0.664	0.000	0.238	6.524	0.047

References

1. Farrell W (1972) Deformation of the earth by surface load. Rev Geophys Space Phys 10: 761-797.
2. Jentzsch G (1997) Earth tides and ocean tidal loading. In: Wilhelm H, Zürn W, Wenzel H-G, Tidal phenomena, lecture notes in earth sciences. Springer, Berlin Heidelberg, 66: 145-167.
3. Ducarme B (2009) Limitations of high precision tidal prediction. Bull Inf Marées Terr 145: 11663-11677.
4. Agnew DC (2015) Earth tides. In: G Schubert, Treatise on Geophysics. (2nd edn), 3: 151-178.
5. Bos MS, Penna NT, Baker TF, Clarke PJ (2015) Ocean tide loading displacements in western Europe: 2. GPS-observed anelastic dispersion in the asthenosphere. J Geophys Res Solid Earth 120: 6540-6557.
6. Llubes M, Mazzega P (1997) Testing recent global ocean tide models with loading gravimetric data. Prog Oceanog 40: 369-383.
7. Baker TF, Bos MS (2003) Validating earth and ocean tide models using tidal gravity measurements. Geophys J Int 152: 468-485.
8. Boy JP, Llubes M, Hinderer J, Florsch N (2003) A comparison of tidal ocean loading models using superconducting gravimeter data. Journal of Geophysical Research 108.
9. Boy JP, Lyard F (2008) High-frequency non-tidal ocean loading effects on surface gravity measurements. Geophys J Int 175: 35-45.
10. Sun HP, Ducarm B, House X, Leslie V, Jianqiao X, et al. (2005) Adaptability of the ocean and Earth tidal models based on global observations of the superconductive gravimeters. Science in China Ser D Earth Sciences 48: 1859-1869.
11. Sun HP, Hsu HT, Chen W, Chen XD, Zhou JC, et al. (2006) Study of the earth's gravity tide and ocean loading characteristics in Hongkong area. Chinese Journal of Geophysics 49: 657-670.
12. Lysaker DI, Breili K, Pettersen BR (2008) The gravitational effect of ocean tide loading at high latitude coastal stations in Norway. J Geod 82: 569-583.
13. Arnoso J, Benavent M, Montesinos FG (2011) [en línea]. Updating gravimetric tide parameters and ocean tide loading corrections at the observing sites Cueva de los Verdes and Timanfaya of the Geodynamics Laboratory of Lanzarote. In: 25 years of scientific activity at the Lanzarote Geodynamic Laboratory. House of the Volcanoes - Cabildo de Lanzarote. 1-20.
14. Hábel B, Meurers B (2014) A new tidal analysis of superconducting gravity observations in Western and Central Europe. Contrib Geophys Geod 44: 1-24.
15. Amoruso A, Crescentini L (2016) Nonlinear and minor ocean tides in the Bay of Biscay from the strain tides observed by two geodetic laser strainmeters at Canfranc (Spain). J Geophys Res Oceans 121: 4873-4887.
16. Amoruso A, Crescentini L (2020) Parameters of the earth's free core nutation from diurnal strain tides. Scientific Reports 10: 9756.

17. Hinderer J, Riccardi U, Rosat S, Boy J, Hector B, et al. (2020) A study of the solid earth tides, ocean and atmospheric loadings using an 8-year record (2010-2018) from superconducting gravimeter OSG-060 at Djougou (Benin, West Africa). J Geodyn 134: 101692.

18. Lambert A, Pagiatakis SD, Billyard AP, Dragert H (1998) Improved ocean tide loading corrections for gravity and displacement: Canada and northern United States. J Geophys Res 103: 30231-30244.

19. Thomas ID, King MA, Clarke PJ (2007) A comparison of GPS, VLBI and model estimates of ocean tide loading displacements. J Geod 81: 359-368.

20. Penna NT, Bos MS, Baker TF, Scherneck HG (2008) Assessing the accuracy of predicted ocean tide loading displacement values. Journal of Geodesy 82: 893-907.

21. Penna NT, Clarke PJ, Bos MS, Baker TF (2015) Ocean tide loading displacements in western Europe: 1. Validation of kinematic GPS estimates. J Geophys Res Solid Earth 120: 6523-6539.

22. Vergnolle, Bouin MN, Morel L, Masson F, Durand S, et al. (2008) GPS estimates of ocean tide loading in NW-France: determination of ocean tide loading constituents and comparison with a recent ocean tide model. Geophys J Int 173: 444-458.

23. Hwang Ch, Huang JF (2013) Numerical modeling of displacements due to ocean tide loading: Case study at GPS stations in Taiwan and western Pacific. Journal of the Chinese Institute of Engineers 36: 1017-1028.

24. Li Z, Jiang W, Ding W, Deng L, Peng L (2014) Estimates of minor ocean tide loading displacement and its impact on continuous GPS coordinate time series. Sensors 14: 5552-5572.

25. Kalita JZ, Rzepecka Z (2015) Impact of ocean tides loading on precise point positioning based on FES2004 model. Artificial Satellites 50: 77-89.

26. Amoruso A, Crescentini L (2009) The geodetic laser interferometers at Gran Sasso, Italy: Recent modifications and correction for local effects. Journal of Geodynamics 48: 120-125.

27. Amoruso A, Botta V, Crescentini L (2012) Free core resonance parameters from strain data: Sensitivity analysis and results from the Gran Sasso (Italy) extensometers. Geophys J Int 189: 923-936.

28. d'Oreye N, Zürn W (2006) Quarter-diurnal tides observed with a long-base water-tube tiltmeter in the Grand Duchy of Luxembourg. Journal of Geodynamics 41: 175-182.

29. Boy JP, Longuevergne L, Boudin F, Jacob T, Lyard F, et al. (2009) Modelling atmospheric and induced non-tidal oceanic loading contributions to surface gravity and tilt measurements. J Geodyn 48: 182-188.

30. Florsch N, Llubes M, Wöppelmann G, Longuevergne L, Boy JP (2009) Oceanic loading monitored by ground-based tiltmeters at Cherbourg (France). J Geodyn 48: 211-218.

31. Mentes G (2008) Observation of recent tectonic movements by extensometers in the Pannonian Basin. J Geodyn 45: 169-177.

32. Mentes G (2010) Quartz tube extensometer for observation of Earth tides and local tectonic deformations at the Sopronbánfalva Geodynamic Observatory, Hungary. Rev Sci Instrum 81: 074501.

33. Van Camp M, Vauterin P (2005) Tsoft: Graphical and interactive software for the analysis of time series and earth tides. Computers & Geosciences 31: 631-640.

34. Wenzel HG (1996) The nanogal Software: Earth tide data processing package Eterna 3.30. Bull Inf Marées Terr 124: 9425-9439.

35. Wahr JM (1981) Body tides on an elliptical, rotating, elastic and oceanless Earth. Geophys J R Astr Soc 64: 677-703.

36. Dehant V (1987) Tidal parameters for an unelastic Earth. Phys Earth Planet Inter 49: 97-116.

37. Hartmann T, Wenzel HG (1995) Catalogue HW95 of the tide generating potential. Bull Inf Marées Terr 123: 9278-9301.

38. Agnew DC (2013) SPOTL: Some programs for ocean-tide loading. Institute of Geophysics and Planetary Physics, Scripps Institution for Oceanography, University of California, USA Technical Report.

39. Bos MS, Scherneck HG (2013) Computation of green's functions for ocean tide loading. In: G Xu, Sciences of Geodesy - ii. Springer, Berlin Heidelberg, 1-52.

40. Harkrider DG (1970) Surface waves in multilayered elastic media Part II. Higher mode spectra and spectral ratios from point sources in plane layered Earth model. Bull Seismol Soc Am 60: 1937-1987.

41. Savcenko R, Bosch W (2012) EOT11a - empirical ocean tide model from multi-mission satellite altimetry. DGFI Report No. 89.

42. Taguchi E, Stammer D, Zahel W (2014) Inferring deep ocean tidal energy dissipation from the global high-resolution data-assimilative HAMTIDE model. J Geophys Res Oceans 119: 4573-4592.

43. Egbert GD, Erofeeva YS (2002) Efficient inverse modeling of barotropic ocean tides. Journal of Atmospheric and Oceanic Technology 19: 183-204.

44. Cheng Y, Andersen OB (2010) Improvement in global ocean tide model in shallow water regions. OSTST Meeting, Lisbon, 18-22.

45. Eanes RJ (1994) Diurnal and semidiurnal tides from TOPEX/POSEIDON altimetry. Eos Transactions American Geophysical Union 75: 108.

46. Lyard F, Lefevre F, Letellier T, Francis O (2004) Modelling the global ocean tides: Modern insights from FES2004. Ocean Dyn 56: 394-415.

47. Le Provost C, Lyard F, Molines J, Genco ML, Rabilloud F (1998) A hydrodynamic ocean tide model improved by assimilating a satellite altimeter-derived data set. J Geophys Res 103: 5513-5529.

48. Schwiderski EW (1980) On charting global ocean tides. Rev Geophys 18: 243-268.

49. Carrère L, Lyard F, Cancet M, Guillot A, Roblou L (2013) FES 2012: A new global tidal model taking advantage of nearly 20 years of altimetry. Proc '20 Years of Progress in Radar Altimetry' 24-29 September 2012, Venice, Italy.

50. Carrère L, Lyard F, Cancet M (2015) FES2014, A new tidal model on the global ocean with enhanced accuracy in shallow seas and in the arctic region. EGU General Assembly, Vienna, Austria, 12-17.

51. Carrère L, Lyard F, Cancet M, Guillot A, Picot N (2016) Finite Element Solution FES2014, a new tidal model - Validation results and perspectives for improvements. Presentation to ESA Living Planet Conference, Prague.

52. Ray RD (1999) A global ocean tide Model from TOPEX/POSEIDON Altimetry: GOT99.2. NASA Technical Memorandum 209478.

53. Kustowski B, Ekström G, Dziewoński AM (2008) Anisotropic shear-wave velocity structure of the Earth's mantle: A global model. J Geophys Res 113.

54. Neumeyer, J del Pino J, Dierks O, Sun HP, P flugH (2005) Improvement of ocean loading correction on gravity data with additional tide gauge measurements. J Geodyn 40: 104-111.

DOI: 10.35840/2631-5033/1844